Analytical approach to particle dissolution in a finite medium

F. J. Vermolen, P. van Mourik, and S. van der Zwaag

An important part in the total production process of extrudable aluminium alloys is the homogenisation treatment of the as cast billets before hot extrusion. During this homogenisation treatment several microstructural changes take place. The most important changes are the dissolution of the precipitates formed during solidification and the homogeneous redistribution of alloying elements. Modelling of the particle dissolution in simple binary systems has recently been achieved by Tundal and Ryum using a numerical model. In their model a moving interface between the particle and the aluminium rich matrix was taken into account as well as the finite size of the cell in which the particles dissolve. Furthermore, conditions of local equilibrium at the particle/matrix interface were assumed at all stages of the dissolution process. This was a significant improvement to earlier analytical models in which the interface was assumed to be stationary. The present work describes the development of a semianalytical model for the dissolution of spherical particles in finite media also assuming a moving boundary. The results of the present semianalytical model are compared to those of the numerical model. A fairly good agreement was obtained for most conditions. At long dissolution times the predictions of the two models deviate due to a simplifying assumption used in the analytical model. *MST/3501*

© 1997 The Institute of Materials. Manuscript received 17 November 1995; in final form 22 February 1996. The authors are at the Laboratory of Materials Science, Delft University of Technology, The Netherlands.

List of symbols

A_n	Fourier constant with index n
B_n	normalisation constant with index n
$c(r, t)$	atomic fraction of element B as a function of time and space
c^m	solid solubility of element B in A at the initial temperature
$c^{\alpha/\beta}$	solid solubility of element B in A
$c^{\beta/\alpha}$	atomic fraction of element B in the particle
c^0	average concentration of element B
$C(r, t)$	atomic fraction of element B relative to the solid solubility at the homogenisation temperature
D	diffusion coefficient of element B in A, $m^2 s^{-1}$
L	average interparticle distance, m
M_A	molar mass of A, kg
M_B	molar mass of element B, kg
n	index
r	distance from the particle centre, m
$R(t)$	particle radius as a function of time, m
R_c	cell radius, i.e. half the distance between two centres of particles, m
R_0	initial particle radius, m
t	annealing time, s
T_{dis}	dissolution temperature, K
T_{eut}	eutectic temperature, K
T_{ini}	initial temperature, K
α_n	eigenvalue, following from boundary conditions with index n
β_n	eigenvalue, following from boundary conditions with index n
θ_n	eigenfunction with index n
λ_n	eigenvalue, following from boundary conditions with index n
ρ_a, ρ_b	densities (Kg mm^{-3}) of elements A, B
$\rho_n(r)$	eigenfunction with index n

Introduction

The microstructure of cast aluminium alloys contains many inhomogeneities, such as intermetallic compounds and precipitates, making the material unsuitable for hot deformation. Homogenisation, by annealing at the temperature of maximal solid solubility, transforms the microstructure of cast alloys into a more appropriate form for hot deformation. During homogenisation, three processes can occur: the dissolution of precipitates; the precipitation of the alloying elements that were in supersaturation after solidification; and the phase transformation of (intermetallic) compounds. The characteristic alloying elements are largely present as precipitates. Homogenisation results in a more uniform distribution of the alloying elements via the dissolution of precipitates and/or intermetallic compounds. Hence, particle dissolution is a very important part in the homogenisation process.

To describe particle dissolution several physical models have been developed, incorporating the effects of long distance diffusion[1,2] and non-equilibrium conditions at the interface.[3] The long distance diffusion models imply that the reaction at the particle/matrix interface proceeds infinitely fast. Therefore, these models provide an upper boundary for the dissolution kinetics. Whelan[1] considered particles dissolving in an infinite medium using the stationary interface approximation. Tundal and Ryum[2] considered the effects of a finite cell size on the dissolution kinetics. Their numerical solution also took the interface mobility into account. In their numerical model the interface was mobile but assumed to be stationary during each time step in the calculations. Using the same set of boundary conditions an analytical approach for this problem is presented in the present paper. The results of this analytical approach are compared with the results obtained by Tundal and Ryum.

Model

The model considers a binary alloy with limited solubility of B atoms in the A rich phase (*see* Fig. 1). For alloys with an average composition c^0, which are in the two phase region at the starting temperature T_{ini}, the system is assumed to consist of equally sized spherical particles of composition $c^{\beta/\alpha}$ in an A rich matrix of uniform composition c^m. Upon raising the temperature to the homogenisation temperature T_{dis} the solubility of the A rich phase increases and the particle starts to dissolve. At all times the matrix

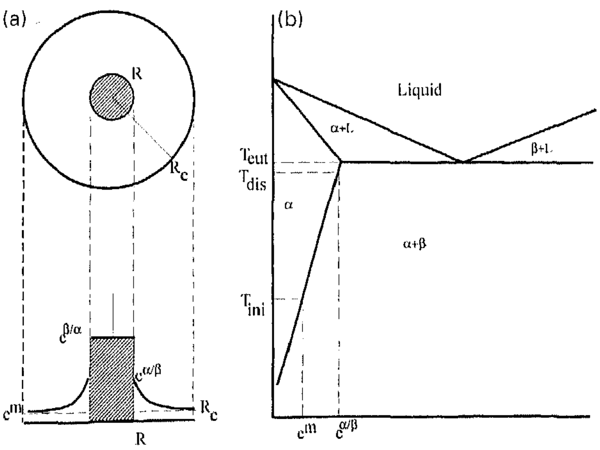

1 ***a*** **spherical particle in spherical cell;** ***b*** **schematic phase diagram for system A–B: see list of symbols for term definitions**

composition at the interface equals the solubility $c^{\alpha/\beta}$, i.e. local equilibrium is imposed. The solubility at the homogenisation temperature is defined as $c^{\alpha/\beta}$.

Assuming a uniform spatial distribution of particles, the average interparticle distance L can be used to calculate the radius of the equivalent spherical cell in which the particle dissolves

$$R_c = \left(\frac{3}{4\pi}\right)^{1/3} L \quad (1)$$

Assuming that the total amount of B atoms in each equivalent cell is constant, the net transfer of B atoms between the cells can be excluded. This implies

$$\frac{\partial c(R_c, t)}{\partial r} = 0 \quad (2)$$

To obtain a homogeneous boundary condition at the interface, it is convenient to substitute $C(r, t) = c(r, t) - c^{\alpha/\beta}$. This substitution will not change equation (1). During dissolution B atoms migrate from the interface. It is assumed that there is no diffusion inside the particle. To maintain the atomic fraction just outside the dissolving particle at $c^{\alpha/\beta}$, the interface reaction has to proceed infinitely fast. Hence, the rate of dissolution is completely determined by the long range diffusion of B atoms in the A rich phase. Application of Fick's second law for a spherical geometry with axial symmetry yields

$$\frac{\partial C(r, t)}{\partial t} = D\left[\frac{\partial^2 C(r, t)}{\partial r^2} + \frac{2}{r}\frac{\partial C(r, t)}{\partial r}\right] \quad (3)$$

$$\forall R < r < R_c, \forall t \geqslant 0$$

where D is the diffusion coefficient of B in A and the value of D is assumed to be independent of composition. The initial boundary value problem, stated by equations (1), (2), and (3), has a solution, if and only if $C(r, t)$ has at least a continuous second derivative with respect to r at the interval $R < r < R_c$ and a continuous first derivative with respect to t for all $t > 0$. Moreover, it can be proven that the solution of equation (3) is unique.[4] As the number of B atoms in the cell is constant, it can be derived that

$$\frac{dR(t)}{dt} = \frac{D}{\left(\frac{\rho_B}{M_B}c^{\beta/\alpha} - \frac{\rho_A}{M_A}c^{\alpha/\beta}\right)}\frac{\rho_A}{M_A}\lim_{r \downarrow R(t)}\frac{\partial C(r, t)}{\partial r} \quad (4)$$

$$\forall t \geqslant 0$$

where ρ_A and ρ_B are the densities of element A and B respectively and M_A and M_B are the molar masses of elements A and B.

From equation (4) it follows that the value of $\partial c(R, t)/\partial r$ determines the value of $dR(t)/dt$. Apparently, the gradient of the composition of B atoms present in the immediate vicinity of the dissolving particle governs the rate of the interface velocity $dR(t)/dt$. The initial boundary value problem combined with equation (5) falls into the class of Stefan problems.[5] To solve equation (3), solutions of the form $C(r, t) = \rho(r)\theta(t)$ are sought. Subsequent substitution into equation (4) and devision by $DC(r, t)$ yields

$$\frac{\theta'(t)}{D\theta(t)} = \frac{\rho''(r) + \frac{2}{r}\rho(r)}{\rho(r)} = -\lambda^2 \quad (5)$$

Since the left and middle sides of equation (5) are functions of t and r respectively, the constant $-\lambda^2$ has been introduced. The constant has to be negative to obtain a non-trivial solution. From equation (5) two ordinary differential equations are obtained

$$\theta'(t) + \lambda^2 D\theta(t) = 0 \quad (6a)$$

$$\rho''(r) + 2r^{-1}\rho'(r) + \lambda^2\rho(r) = 0 \quad (6b)$$

with respective solutions

$$\theta(t) = A\exp(-D\lambda^2 t) \quad (7a)$$

$$\rho(r) = Br^{-1}\cos(\lambda r - \alpha) \quad (7b)$$

where A and B are integration constants and α and λ are eigenvalues. If the interface is assumed to be instantaneously stationary, it follows from substitution of $C(r, t) = \rho(r)\theta(t)$ into the boundary conditions given by equations (1) and (2) that

$$\rho(R) = 0 \quad (8a)$$

$$\frac{d\rho(R_c)}{dr} = 0 \quad (8b)$$

Substitution of equation (7b) into the boundary conditions (*see* equation (8)) yields for sets of λ and α

$$\lambda_n R - \alpha_n = \frac{\pi}{2}(2n + 1) \quad (9a)$$

$$\tan(\lambda_n R_c - \alpha_n) = -\frac{1}{\lambda_n R_c} \quad (9b)$$

$$\forall n \in Z$$

From equation (9) the constants λ_n and α_n can be determined. For each n, there is a function $\rho_n(r)$ (*see* equation (7b)) satisfying equations (6b) and (8b). The linear combination of the set $\{\rho_n(r)\}$ satisfies equations (6b) and (8b). Thus, for the concentration as a function of time and distance from the particle centre, it follows

$$C(r, t) = \sum_{n=-\infty}^{\infty}\left[A_n B_n \exp(-\lambda_n^2 Dt)\frac{\cos(\lambda_n r - \alpha_n)}{r}\right] \quad (10)$$

The constants A_n and B_n have to be determined. Multiplication of equation (6b) by r^2, yields for each $\rho(r)$

$$\frac{d}{dr}\left(r^2\frac{d\rho_n(r)}{dr}\right) + \lambda_n^2 r^2 \rho_n(r) = 0 \quad (11)$$

The combination of equations (8) and (10) falls into the class of the Sturm–Liouville systems[6,7] with eigenvalues λ_n and α_n (as given in equation (9)). Multiplication of equation (11) for two different values of n, i, and j with $\rho_j(r)$ and $\rho_i(r)$ respectively, subtraction and integration over the interval $R < r < R_c$ reveals that the set of functions $\{\rho(r)\}$ are orthogonal with respect to r^2. Substitution of $t = 0$, the initial situation, into equation (10), yields

$$c^{\mathrm{m}} - c^{\alpha/\beta} = \sum_{\mathrm{n}=-\infty}^{\infty} A_{\mathrm{n}} \rho_{\mathrm{n}}(r) \quad . \; . \; . \; . \; . \; . \; . \; . \; . \; (12)$$

It is convenient to determine the coefficients B_{n} such that the functions $\rho(r)$ are orthonormal, that is

$$\int_{\mathrm{R}}^{\mathrm{R_c}} r^2 \rho_{\mathrm{n}}(r) \rho_{\mathrm{m}}(r) \, \mathrm{d}r = \delta_{\mathrm{nm}}$$

in which δ_{nm} represents the Kronecker delta, because each (piecewise) continuous function can be decomposed into an infinite linear combination of orthonormal eigenfunctions. Then, from the orthonormality of the set of functions $\{\rho(r)\}$ and equation (12), the coefficients A_{n} are determined by

$$A_{\mathrm{n}} = (c^{\mathrm{m}} - c^{\alpha/\beta}) \int_{\mathrm{R}}^{\mathrm{R_c}} r^2 \rho_{\mathrm{n}}(r) \, \mathrm{d}r \quad . \; . \; . \; . \; . \; . \; . \; . \; (13)$$

Evaluation of the integral and substitution of equation (9) into equation (13), yields for the coefficients A_{n}

$$A_{\mathrm{n}} = (c^{\alpha/\beta} - c^{\mathrm{m}}) B_{\mathrm{n}} \frac{R}{\lambda_{\mathrm{n}}} (-1)^{\mathrm{n}} \quad . \; . \; . \; . \; . \; . \; . \; . \; . \; (14)$$

The orthonormality of the functions $\rho(r)$ requires for the coefficients B_{n}

$$B_{\mathrm{n}} = \left[\frac{2\lambda_{\mathrm{n}}}{\lambda_{\mathrm{n}}(R_{\mathrm{c}} - R) - \dfrac{\cos^2(\lambda_{\mathrm{n}} R_{\mathrm{c}} - \alpha_{\mathrm{n}})}{\lambda_{\mathrm{n}} R_{\mathrm{c}}}} \right]^{1/2} \quad . \; . \; . \; . \; . \; (15)$$

Combination of equations (10), (13), and (14), using the backward substitution $c(r, t) = C(r, t) + c^{\alpha/\beta}$, and some elementary algebra yield

$$c(r, t) = c^{\alpha/\beta} + \frac{2R(c^{\alpha/\beta} - c^{\mathrm{m}})}{r} \times \sum_{\mathrm{n}=-\infty}^{\infty} \left\{ \frac{(-1)^{\mathrm{n}}(1 + \lambda_{\mathrm{n}}^2 R_{\mathrm{c}}^2) \cos(\lambda_{\mathrm{n}} r - \alpha_{\mathrm{n}}) \exp(-\lambda_{\mathrm{n}}^2 Dt)}{\lambda_{\mathrm{n}}[(R_{\mathrm{c}} - R)(1 + \lambda_{\mathrm{n}}^2 R_{\mathrm{c}}^2) - R_{\mathrm{c}}]} \right\} \quad . \; . \; . \; . \; . \; . \; . \; . \; . \; . \; (16)$$

Substitution of equation (16) into equation (4) yields the following equation for the interface velocity

$$\frac{\mathrm{d}R(t)}{\mathrm{d}t} = -2Dk \sum_{\mathrm{n}=-\infty}^{\infty} \left\{ \frac{(1 + \lambda_{\mathrm{n}}^2 R_{\mathrm{c}}^2) \exp(-\lambda_{\mathrm{n}}^2 Dt)}{[(R_{\mathrm{c}} - R)(1 + \lambda_{\mathrm{n}}^2 R_{\mathrm{c}}^2) - R_{\mathrm{c}}]} \right\} \quad . \; . \; . \; . \; . \; . \; . \; . \; . \; (17a)$$

in which k is defined as

$$k = \frac{c^{\alpha/\beta} - c^{\mathrm{m}}}{\dfrac{\rho_{\mathrm{B}}}{M_{\mathrm{B}}} \dfrac{M_{\mathrm{A}}}{\rho_{\mathrm{A}}} c^{\beta/\alpha} - c^{\alpha/\beta}} \quad . \; . \; . \; . \; . \; . \; . \; . \; . \; . \; (17b)$$

As far as is known, equation (17) is the first semianalytical equation to describe the dissolution with equilibrium at the particle's interface in a finite cell with radius R_{c} with $\infty > R_{\mathrm{c}} > R_0$. According to equation (17), the kinetics of dissolution $\mathrm{d}R(t)/\mathrm{d}t$ depend on $c^{\alpha/\beta}$, $c^{\beta/\alpha}$, and c^{m}, and the long distance volume diffusion coefficient. The factor on the right hand side of the summation symbol results from the geometrical and physical constraints: dissolving has to take place in a finite space while fulfilling the law of mass conservation, i.e. the amount of B atoms in the cell remains constant during dissolution. Furthermore, it follows that for increasing annealing time t, $|\mathrm{d}R^2(t)/\mathrm{d}t|$ decreases continuously and uniformly, implying that for very small dissolution times $|\mathrm{d}R^2(t)/\mathrm{d}t|$ is maximal, as can be expected intuitively. It can be shown that for $t \downarrow 0$, the value of $\mathrm{d}R^2(t)/\mathrm{d}t$ and $\mathrm{d}R(t)/\mathrm{d}t$ does not depend on R_{c} (*see* Appendix). Clearly, in the first stages of homogenisation, the dissolution proceeds as if the cell size were infinite.

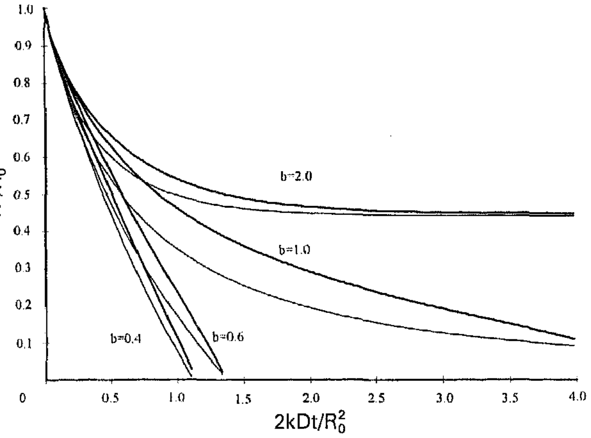

2 Values of normalised particle area (R^2/R_0^2) as function of normalised dissolution time ($2kDt/R_0^2$) with $k = 0{\cdot}01$ for various values of *b* where *k* and *b* are defined by equations (17b) and (19) respectively: thick lines indicate results of semianalytical model; thin lines indicate corresponding results of Tundal and Ryum approach

Since the eigenvalues λ_{n} and α_{n} are taken for a constant position of the given boundary condition at the interface, the eigenvalues have to be calculated for each value of $R(t)$. From this, it is obvious that if the eigenvalues are known, equation (17) can only be solved numerically. Combination of both parts of equation (9) yields

$$\frac{1}{\lambda_{\mathrm{n}} R_{\mathrm{c}}} + \tan\left[\frac{\pi}{2}(2n + 1) + \lambda_{\mathrm{n}}(R_{\mathrm{c}} - R)\right] = 0 \quad . \; . \; . \; (18)$$

From equation (18) the eigenvalues λ_{n} can be calculated for each value of R by the Newton–Raphson zero point iteration method[7] with an accuracy only limited by computer capacity. Subsequent substitution into equation (9) yields the eigenvalues α_{n}. By substitution of the eigenvalues into equation (17), the interface velocity $\mathrm{d}R(t)/\mathrm{d}t$ can be calculated. The value of R can be obtained by numerical integration of equation (17) applying a Runge–Kutta method.[8]

Results and discussion

The dissolution of the spherical particle has been calculated for a number of different starting conditions characterised by the parameter k, which is a measure for the concentration difference between interface and matrix, *see* equation (17b), and b, which is a measure of the possibility of full particle dissolution at infinite annealing times and which is defined as

$$b = \frac{c^0 - c^{\mathrm{m}}}{c^{\alpha/\beta} - c^{\mathrm{m}}} \quad . \; . \; . \; . \; . \; . \; . \; . \; . \; . \; . \; . \; . \; (19)$$

The normalised particle area R^2/R_0^2 is plotted in Figs. 2 and 3 as a function of the normalised dissolution time $2kDt/R_0^2$ for various values of b for $k = 0{\cdot}01$ and $k = 0{\cdot}25$ respectively. The results of the calculations based on the analytical solution are indicated by the thick lines. The figures show that the dissolution rate has a maximal value at $t = 0$ and that the dissolution rate decreases continuously during the dissolution process. The decrease in dissolution rate is due to the finite dimensions of the cell in which the particle dissolves. In the case of particle dissolution in an infinite cell with a stationary concentration profile a linear

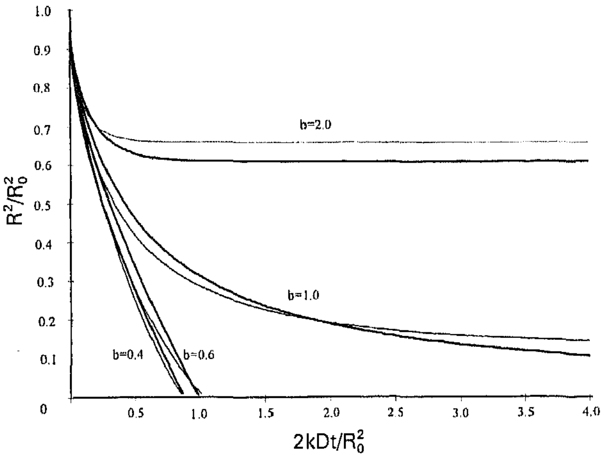

3 Values of R^2/R_0^2 as function of $2kDt/R_0^2$ with $k=0{\cdot}25$ for various values of b: thick lines indicate results of semianalytical model; thin lines indicate corresponding results of Tundal and Ryum approach

dependence between the particle area and the dissolution time exists.

Furthermore, both figures show that for values of $b<1$, the particle dissolves completely, as is to be expected. The dissolution time increases rapidly when b approaches 1. For values of $b>1$ the particle dissolution is incomplete but the final state is obtained after a relatively short annealing time. The final particle size depends on b. Comparison of the curves of Figs. 2 and 3 shows that the dissolution kinetics do not vary strongly with k when plotted against the normalised time $2Dkt/R_0^2$. Of course, when plotted against the time t the dissolution rate will accelerate with increasing k value or increasing concentration gradient.

The dissolution kinetics predicted by the semianalytical approach have been compared to those predicted using the numerical approach for particle dissolution as developed by Tundal and Ryum.[2] The results of these calculations, using the same set of k and b values as for the calculations with the analytical model, are also shown in Figs. 2 and 3 respectively. The results of the numerical model are indicated by the thin lines. For small dissolution times both dissolution rates coincide. However, for larger dissolution times it can be seen that the analytical approach and the numerical deviate. The deviations between the analytical and numerical approach are caused by the assumption underlying equation (12). This can be explained as follows: for each iteration step in the calculation the position of the interface, i.e. the boundary condition, changes. Formally, a new boundary value problem should be introduced at each time step, in which the initial condition is not given by $c^{\mathrm{m}}-c^{\alpha/\beta}$ but by the concentration profile during the last iteration step. This means that equation (12) has to be changed to

$$c(r,t)-c^{\alpha/\beta}=\sum_{n=-\infty}^{\infty}\tilde{A}_n\rho_n(r) \quad . \; . \; . \; . \; . \; . \; . \; . \; . \quad (20)$$

where $\tilde{A}_n$ represents the integration coefficients at the time $t+$timestep. From this and the orthonormality it follows that the coefficients $\tilde{A}_n$ can be determined by

$$\tilde{A}_n=\int_R^{R_c}[c(r,t)-c^{\alpha/\beta}]\rho_n(r)r^2\,\mathrm{d}r \quad . \; . \; . \; . \; . \; . \quad (21)$$

Such a modification would result in a significant extension of the computation time. However, equations (12) and (13) provide a good approximation as long as the concentration profile in the A rich phase has not changed significantly. This effect of the deviation of the concentration profile becomes more important as the dissolution proceeds and the concentration profile changes. In the numerical approach for each time step, the concentration profile from the last iteration is used as the initial condition for the new boundary value problem as introduced by the movement of the interface position. The time at which the concentration profile changes significantly becomes smaller as the ratio between the initial particle size and the cell size becomes smaller. That is the reason why for large b values the deviation between the dissolution rates, as predicted by the analytical approach and the numerical approach, starts earlier. The dissolution times predicted by the analytical approach are most accurate for small b values.

Conclusions

A semianalytical model has been derived for the dissolution of spherical particles in finite media assuming that long distance diffusion is the only rate limiting step. The model allows the prediction of the dissolution kinetics as a function of the initial concentration differences between particle and matrix and the interface concentration during dissolution. The model is applicable to the case of complete dissolution and to the case of incomplete dissolution. The predictions of the dissolution kinetics by the analytical model in its present form correspond well with those of a more complex numerical model, provided that the final concentration in the matrix does not differ significantly from the initial concentration profile.

Appendix

At $t=0$, the concentration profile can be written as

$$c(r,t=0)=c^{\beta/\alpha}-(c^{\beta/\alpha}-c^{\mathrm{m}})u(r-R) \quad . \; . \; . \; . \; . \quad (22)$$
$$\forall\, 0\leqslant r\leqslant R_{\mathrm{c}}$$

with

$$u(\tau)=\begin{cases}1\,\forall\,\tau\geqslant 0\\ 0\,\forall\,\tau<0\end{cases}$$

Differentiation of equation (22) and using

$$u(\tau)=\int_{-\infty}^{\tau}\delta(\theta)\,\mathrm{d}\theta$$

with $\delta(\theta)$ the unit pulse function, yields for the concentration gradient at $t=0$

$$\frac{\partial c(r,t=0)}{\partial r}=-(c^{\beta/\alpha}-c^{\mathrm{m}})\delta(r-R) \quad . \; . \; . \; . \; . \; . \quad (23)$$

Substitution of equation (23) into equation (4)

$$\frac{\mathrm{d}R(t=0)}{\mathrm{d}t}=-\frac{c^{\beta/\alpha}-c^{\mathrm{m}}}{\dfrac{\rho_{\mathrm{B}}}{M_{\mathrm{B}}}c^{\beta/\alpha}-\dfrac{\rho_{\mathrm{A}}}{M_{\mathrm{A}}}c^{\alpha/\beta}}D\frac{\rho_{\mathrm{A}}}{M_{\mathrm{A}}} \quad . \; . \; . \; . \quad (24)$$

Equation (24) shows that the initial interface velocity $\mathrm{d}R(t=0)/\mathrm{d}t$ is independent of the cell size, as can be expected intuitively.

References

1. M. J. WHELAN: *Met. Sci.*, 1969, **3**, 95–97.
2. U. H. TUNDAL and N. RYUM: *Metall. Trans. A*, 1992, **23A**, 433–444.
3. F. V. NOLFI, Jr, P. G. SHEWMON, and J. S. FOSTER: *Trans. AIME*, 1969, **245**, 1427–1433.
4. D. W. TRIM: 'Applied partial differential equations', 1st edn, 205–206; 1990, Boston, MA, PWS Kent.

5. D. G. WILSON, A. D. SOLOMON, and P. T. BOGGS: 'Moving boundary problems', 1st edn, 25–41; 1978, New York, NY, Academic Press.
6. D. W. TRIM: 'Applied partial differential equations', 1st edn, 141–168; 1990, Boston, MA, PWS Kent.
7. M. ABRAMOWITZ and I. A. STEGUN: 'Handbook of mathematical functions', 18; 1962, New York, NY, Dover Publications.
8. M. ABRAMOWITZ and I. A. STEGUN: 'Handbook of mathematical functions', 896; 1962, New York, NY, Dover Publications.